Aerosol and Air Quality Research, 17: 2705–2714, 2017

ISSN: 1680-8584 print / 2071-1409 online
doi: 10.4209/aaqr.2016.12.0574

Application of Gas Cyclone–Liquid Jet Absorption Separator for Flue-Gas Desulfurization

Yi-Mou Wang, Xue-Jing Yang, Peng-Bo Fu, Liang Ma*, An-Lin Liu, Meng-Ya He

School of Mechanical and Power Engineering, East China University of Science and Technology, Shanghai 200237, China

ABSTRACT

A gas cyclone–liquid jet absorption separator integrates the functions of cyclone separation, liquid jet atomization, and absorption separation. This study employed this device to conduct a wet flue-gas desulfurization experiment on a gas mixture consisting of air in room temperature and sulfur dioxide (SO_2) to explore this device's prospect of tail gas purification. Sodium hydroxide (NaOH) and sodium carbonate (Na_2CO_3) solutions at various concentrations were used as absorbents under room temperature. The changes in the SO_2 removal efficiency and air pressure drop were investigated with parameters including total gas flow, SO_2 concentration in the flue gas, and absorbent flow. The SO_2 removal efficiency increased to a certain extent as the absorbent concentration, total gas flow, and absorbent flow increased. The maximum SO_2 removal efficiencies of NaOH and Na_2CO_3 were 85% and 77%, respectively. Under identical experimental conditions, the changes in SO_2 removal efficiencies of NaOH and Na_2CO_3 exhibited essentially identical trends, in which NaOH exhibited a 5%–8% greater SO_2 removal efficiency than Na_2CO_3.

Keywords: Flue-gas desulfurization; Cyclonic separation; Jet flow; Absorption separation.

INTRODUCTION

According to the United Nations Environment Programme estimate, the global annual sulfur dioxide (SO_2) emissions are approximately 100 million tons, of which approximately 20 million tons are emitted in China (Klimont *et al.*, 2013). Currently over 200 desulfurization techniques exist that can be divided into three kinds according to before, during, or after combustion (Vincent *et al.*, 2012; Peng *et al.*, 2016). Among these methods, wet desulfurization is mature, efficient, and relatively easy to operate. It has been developed to second and third generations, accounts for up to 85% of the market share in the desulfurization industry, and has been the research focus in current studies on desulfurization technology (Chang *et al.*, 2004; Lian *et al.*, 2004; Pisani and Moraes, 2004).

Bjerle *et al*. (1972) examined the effect of limestone dissolution on SO_2 absorption using a laminar jet tower, and Uchida and Ariga (1985) studied wet desulfurization through a stirred reactor. Brogren and Karlsson (1997) constructed a utility boiler desulfurization system model on the basis of chemiosmosis. Sada *et al*. (1981) examined the mass transfer enhancement process of magnesium sulfate on limestone desulfurization using a double stirring reactor, and analysed the enhancement process on the basis of a double response surface model. Dudek *et al*. (1999) reconstructed the tower foundation under the flue gas inlet of a desulfurization absorption tower, and designed the tower base with an inclination of 30° to numerically simulate the flow field. Strock and Gohara (1994) investigated the effect of factors such as liquid-phase suspension, liquid-phase distribution, and flue gas velocity in the sieve plate column on desulfurization efficiency through a sieve sprinkler modelled in 1:8 scale. Watson *et al*. (1999) attempted to add a canopy over the flue gas inlet in the desulfurization tower to obtain a more uniform flow field distribution. Currently, the main instruments used in wet desulfurization include rotating packed beds, impinging stream reactors, and absorption towers, and the desulfurization rates of these three instruments are ≥ 80%, ≥ 90%, and 68%–90%, respectively (Chang *et al.*, 2011; Gong and Yang, 2011; Wang *et al.*, 2015; Kobayashi *et al.*, 2016). Absorption towers are widely used in the desulfurization industry, but they exhibit problems such as a large land area required, high operation cost, and equipment corrosion and fouling (Michalski, 2000; Bao *et al.*, 2012; Zhu *et al.*, 2015). Although some wet flue-gas desulfurization (WFGD) technologies are available, more cost-effective and efficient equipment and technologies still need to be developed for the industry environment.

A gas cyclone–liquid jet absorption separator harnesses the coupling effect of liquid jet and gas cyclone flow fields to substantially increase the contact area between the gas

* Corresponding author.
Tel.: +86-21-64252748; Fax: +86-21-64251894
E-mail address: maliang@ecust.edu.cn

and liquid without altering the gas–liquid cyclonic separation effect, continuously renewing the absorptive material on the droplet interface. It increases the mass transfer coefficient of the effective interfacial area and maintains the continuous absorption of the droplet interface of the gas, thereby improving the desulfurization efficiency. This study conducted an WFGD experiment using a gas cyclone–liquid jet absorption separator with sodium hydroxide (NaOH) and sodium carbonate (Na_2CO_3) as the alkali absorbent. A novel WFGD technique employing the aforementioned device was developed for actual industrial applications by investigating the effects of parameters such as various concentrations of absorbents, sulfur content in the flue gas, and flow rates of flue gas and absorbents on the SO_2 removal efficiency of the gas cyclone–liquid jet absorption separator.

EXPERIMENT

Gas Cyclone–Liquid Jet Absorption Separator

The gas cyclone–liquid jet absorption separator improves on the cyclone separator design by adding jet holes on the cylinder. In addition, the cylinder structure, the cone structure, inlet, and central exhaust pipe were optimized to integrate the coupling effect of the liquid–gas flow, and the absorption and separation functions.

The total length of the device (H) was 900 mm. The lengths of the upper cylinder (H_1), cone (H_2), and lower cylinder (H_3) sections were 500 mm, 350 mm, and 100 mm, respectively; the upper (D_1), and lower (D_2) diameters were 100 mm, and 45 mm, respectively. The upper cylinder and the outer tube formed a jacket with a 110 mm diameter (D_j). The absorbent was injected through four inlet openings uniformly distributed in the middle section of the jacket to produce radially stabilised axisymmetric jets toward the central axis of the separator. The length of the upper cylinder jet holes section (h) was 290 mm. Eight circular holes with diameters (d) of 2 mm were uniformly distributed in each of the 30 circles, which had an axial distance (l) of 10 mm and a rotation angle of 15°. The cross-sectional shapes of the inlet of typical cyclone separators are usually circular or rectangular. Cui *et al*. (2010), Ma *et al*. (2013) and Zhang *et al.* (2016) reported that a narrow rectangular inlet (with the long side parallel to the cyclone axis) can improve the separation efficiency. In this study, a rectangular inlet with length and width of a = 55 mm and b = 25 mm, respectively, was adopted. The main design parameters of the central exhaust pipe consisted of the insertion depth (S) and pipe diameter (D_x). Previous studies have revealed D_x/D_1 = 0.25–0.5 as a suitable range for the central exhaust pipe (Ma *et al.*, 2014; Zhang *et al.*, 2016), and the present study adopted 0.45 for the D_x/D_1 ratio (i.e., D_x = 45mm). In addition, the present study adopted 0.7 for the S/H ratio (i.e., S = 630 mm) suggested in Bogodage *et al*. (2016) and Safikhani and Mehrabian (2016).

Figs. 1(a) shows the structure size parameters of the device. To facilitate the observation clarity of the gas–liquid contact reaction and the reaction degree, the gas cyclone–liquid jet absorption separator was manufactured with organic glass, as shown in Figs. 1(b).

Wet Flue-Gas Desulfurization Experiment

The WFGD experimental system in this study consisted of a gas cyclone–liquid jet absorption separator, an air blower, a liquid circulation pump, a liquid circulation tank, liquid and gas flowmeters, liquid and gas pressure gauges, and a U-shaped manometer. In addition, laboratory standard SO_2 gas, NaOH solution, and Na_2CO_3 solution were used. Fig. 2 and Table 1 show the experimental system and the equipment information.

In this experiment, the flue gas was simulated with a mixture of ambient air and SO_2. Prior to the experiment, 15 L of absorbent at a predetermined concentration (c_L) was poured into the circulation tank and stirring, and the circulation pump was opened to transfer the absorbent flow (Q_L) to the jacket in the separator at an initial flow rate. The pressurized absorbent generated radially stabilised axisymmetric jets through the jet holes while adjusting the gate at the bottom to form liquid-sealing to ensure a stable discharge of the mixed gas through the central exhaust pipe for at least 5 min. At the beginning of the experiment, the mixed gas was injected at a predetermined flow rate (Q_G) and entered the gas cyclone–liquid jet absorption separator tangentially through the inlet to form a strong cyclonic absorption reaction. Subsequently, the purified gas was discharged from the central exhaust pipe, and the sulfide-containing absorbent flowed out from the bottom of device into the circulation tank. The experiment was conducted at room temperature. The intermittent operations consisted 20-min experiments and the SO_2 removal efficiency and corresponding parameters were measured every 10 min under the stable state. Each experiment was repeated at least 5 times, and the mean value was used as the experimental result.

Experimental Principle and Methodology

In this experiment, the NaOH and Na_2CO_3 solutions absorbed the SO_2 in the mixed gas, and NaOH was used as the absorbent to explain the experimental principle of the gas cyclone–liquid jet absorption separator. The desulfurization process was essentially the mass transfer process of SO_2 and the process of material diffusion. The mechanism can be explained by the two-film theory (Sai *et al.*, 2010; Sun *et al.*, 2010; Zhang *et al.*, 2016).

When the mixed gas (containing SO_2) entered the top of the separator through the tangential inlet, a strong cyclonic field was formed. Simultaneously, the absorbent entered the jacket and was ejected through the holes in the middle section under pressure, and the streamlined absorbent was radially sprayed into the separator to form numerous droplets through continuous impact, collision, and separation with the mixed gas under high-speed tangential rotation (Fig. 3). The SO_2 molecules moved, diffused, and came into contact rapidly with the outer edges of the absorbent droplets, as shown in Figs. 4(a). After the transient reaction, the SO_2 molecules dissolved and were diffused on the droplet surfaces and reacted with the droplets continuously, as shown in Figs. 4(b). Subsequently, the SO_2 molecules formed sulfurous acids after reaching the liquid films from the droplet surfaces, and reacted with NaOH or sodium sulfite (Na_2SO_3). Through the coupling effect of gas and liquid flow fields in the

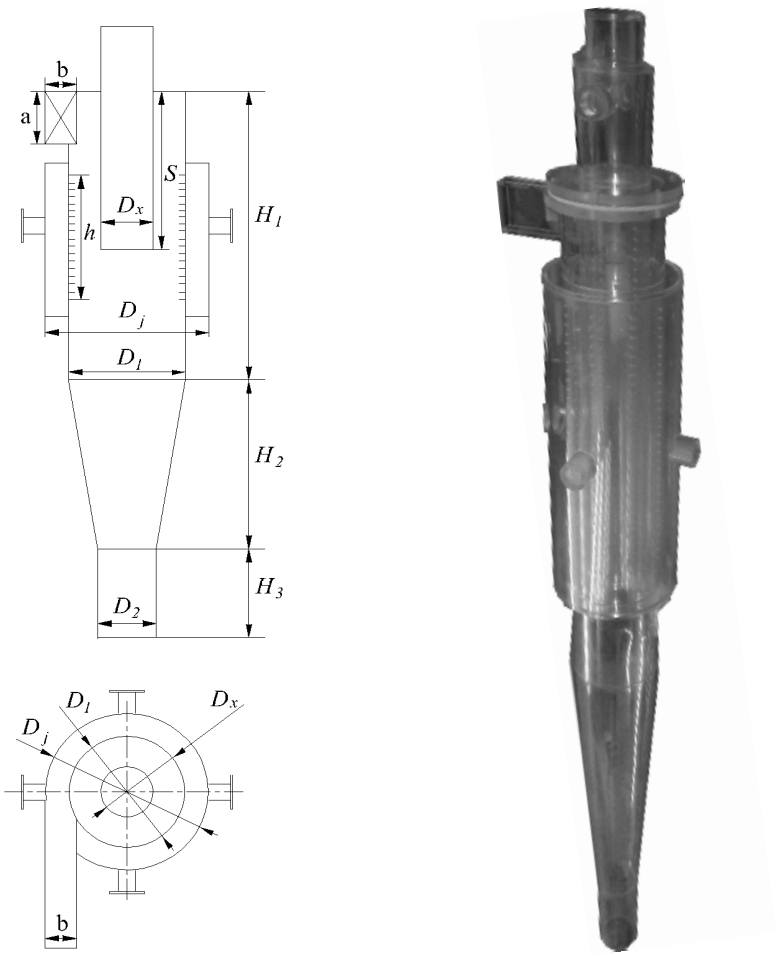

(a) Dimension figure (b) Real figure

Fig. 1. Gas cyclone–liquid jet absorption separator (a. Dimension figure, b. Real figure).

separator, the absorption and reaction process was completed, as shown in Figs. 4(c).

The main chemical equation in the process is:

$$2NaOH + SO_2 \rightarrow Na_2SO_3 + H_2O \quad (1)$$

Consequently, the generated Na_2SO_3 reabsorbed SO_2 as in the following equation:

$$Na_2SO_3 + SO_2 + H_2O \rightarrow 2NaHSO_3 \quad (2)$$

The overall reaction equation is thus:

$$NaOH + SO_2 \rightarrow NaHSO_3 \quad (3)$$

This experiment measured the SO_2 content in the purified flue gas through an SO_2 detector and calculated the SO_2 removal efficiency of the novel separator, η, as follows:

$$\eta = \frac{c_{SG,in} - c_{SG,out}}{c_{SG,in}} \times 100\% \quad (4)$$

where $c_{SG,\ in}$ and $c_{SG,\ out}$ are the concentrations of injected and purified SO_2 in mg m^{-3}, respectively.

RESULTS AND DISCUSSION

Effect of Absorbent Concentration on SO_2 Removal Efficiency

This study examined the effects of absorbent concentration on SO_2 removal efficiency when the total gas flow, inlet SO_2 concentration, and absorbent flow rate were controlled and held constant and the total amount of absorbent was greater than the amount required for the SO_2 reaction. Fig. 5 illustrates the experimental results and demonstrates that the SO_2 removal efficiency increased as the absorbent concentration increased. When the absorbent concentration reached ≥ 8000 g m^{-3}, the change in η flattened out. The maximum η when NaOH and Na_2CO_3 were used as the absorbents were 81.7% and 74.1%, respectively. In addition, the SO_2 concentration in the tail gas decreased as the absorbent concentration increased. When the absorbent concentration increased to ≥ 8000 g m^{-3}, the change in the SO_2 concentration in the tail gas stabilised. The minimum SO_2 concentrations when NaOH and Na_2CO_3 were used as the absorbents were 517 mg m^{-3} and 366 mg m^{-3}, respectively. As the absorbent droplets generated by the cyclonic flow field

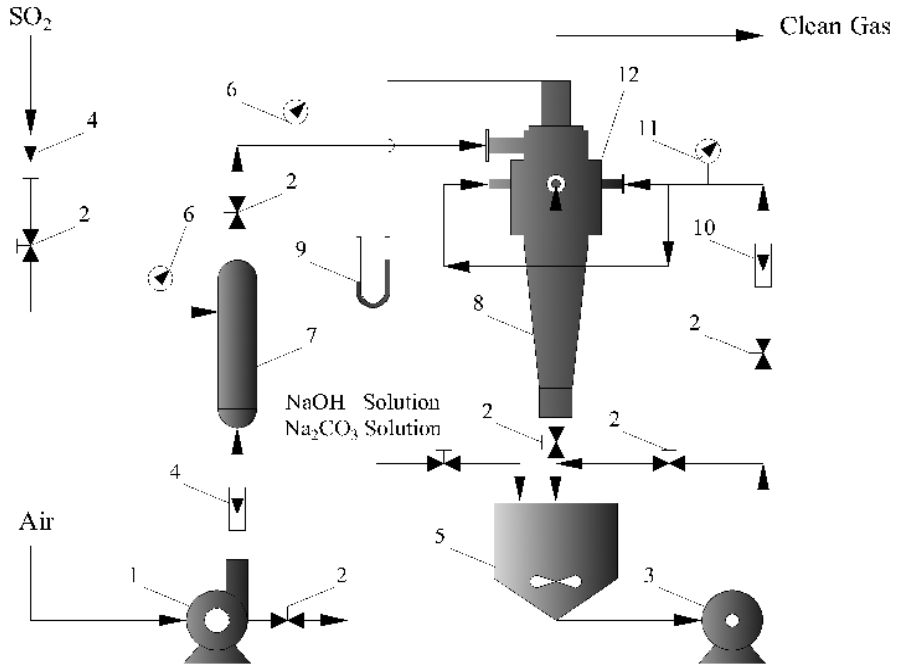

1: air blower; 2: gate; 3: circulation pump; 4: gas flowmeter; 5: circulation tank;
6: air pressure gauge; 7: gas mixing tank; 8: gas cyclone–liquid jet absorption separator;
9: U-shaped manometer; 10: liquid flowmeter; 11: liquid pressure gas; 12: jacket

Fig. 2. Novel WFGD experimental system.

Table 1. Equipment information of the experimental system.

Equipment	Name	Model Number	Quantity	Range	Accuracy Class	Material
SO_2 Flowmeter	Rotor Flowmeter	LZB-4WB	1	0.3–3 L min^{-1}	0.1	Anticorrosion Glass
Gas Flowmeter	Vortex Flowmeter	KKF83E	1	35–350 m^3 h^{-1}	1.0	Metal
Gas Pressure Gauge	Dwyer Pressure Gauge	DPGA-04	1	0–5 psi	0.002	Metal
Liquid Pressure Gauge	Dwyer Pressure Gauge	DPGA-04	1	0–5 psi	0.002	Metal
Liquid Flowmeter	Rotor Flowmeter	LZB-25F	1	100–1000 L h^{-1}	20	Anticorrosion Glass
Air Blower	GOORUI Air Blower	GHBH 001	1	0–175 m^3 h^{-1}	—	Metal
Circulation Pump	Magnetic Pump	20CQ-12	1	0–3 m^3 h^{-1}	—	Stainless Steel
U-shaped Manometer	U-shaped Manometer	—	1	0–6000 Pa	5	Glass
SO_2 Detector	SO_2 Detector	TH2000-SO2	1	0–2000 ppm	1	Metal
Ion Chromatograph	Ion Chromatograph	DX-600	1	—	≤ 2%	—

increased, the reaction opportunities between the gas molecules and absorbent droplets rapidly increased. When the absorbent concentration was low (i.e., < 8000 g m^{-3}), the number of droplets per unit area fell and absorbed fewer SO_2 molecules, resulting in a high SO_2 concentration in the tail gas and a low η; when the absorbent concentration was ≥ 8000 g m^{-3}, the number of droplets reached saturation in SO_2 absorption per unit area, resulting in the minimum SO_2 concentration in the tail gas and the maximum η.

Effect of Inlet SO_2 Concentration on SO_2 Removal Efficiency

This study examined the effects of inlet SO_2 concentration on SO_2 removal efficiency when the total gas flow, absorbent flow, and absorbent concentration (8000 g m^{-3}) were controlled and held constant and the total amount of the absorbent was always greater than the amount required for the SO_2 reaction. Fig. 6 illustrates the experimental results and demonstrates that η continued to decrease as the inlet SO_2 concentration increased from 1500 mg m^{-3} to 5000 mg m^{-3}. The maximum η when NaOH and Na_2CO_3 were used as the absorbents were 83.2% and 76.5%, respectively. The SO_2 concentration in the tail gas increased as the inlet SO_2 concentration increased. The maximum SO_2 concentrations when NaOH and Na_2CO_3 were used as the absorbents were 1106 mg m^{-3} and 1554 mg m^{-3}, respectively. When NaOH was used as the absorbent, increasing the inlet SO_2 concentration yielded third soluble products such as Na_2SO_3

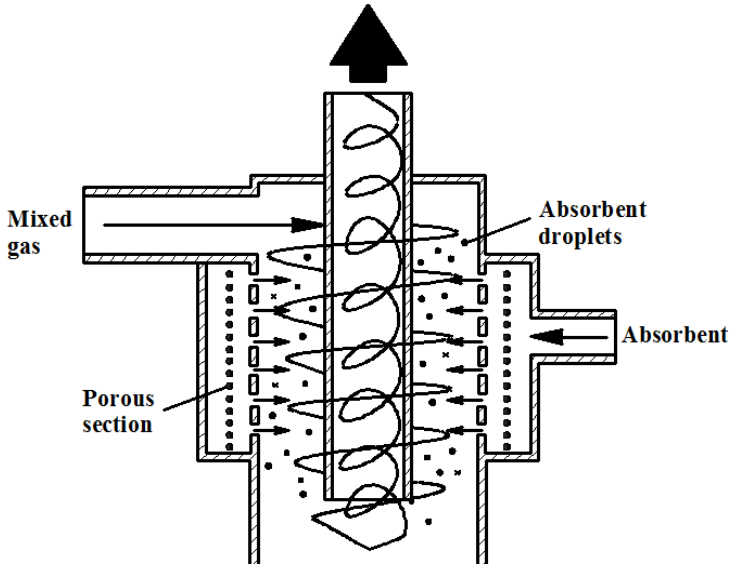

Fig. 3. Droplets formed by gas–liquid interaction.

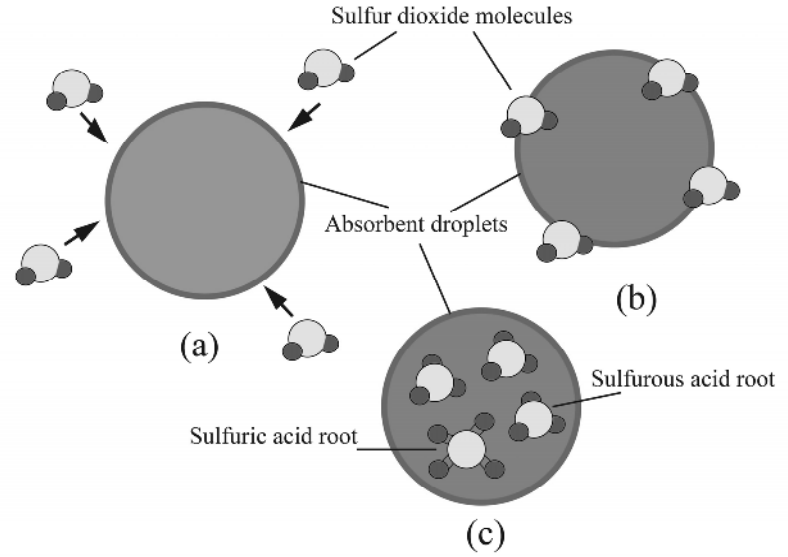

Fig. 4. Interaction between SO_2 and droplets.

and $NaHSO_3$, and Na_2SO_3 continued to react with SO_2. According to Eqs. (1)–(3), a portion of SO_2 reacted with Na_2SO_3 and the molar ratio between the reactants decreased from 2:1(SO_2 reacted with NaOH) to 1:1(SO_2 reacted with Na_2SO_3). Qin *et al*. (2016) argued that a decreased molar ratio between the reactants decreases the SO_2 removal efficiency and increases the SO_2 concentration in the flue gas. In addition, the absorption reaction continues to yield by-products that decrease the absorbent concentration per unit volume of liquid. SO, the insufficient mass transfer force of the SO_2 absorption reaction results in a continuously decreasing of SO_2 removal efficiency.

Ion analysis of the NaOH and Na_2CO_3 absorbents was conducted using the DX-600 ion chromatography system after the absorption reaction. The total gas and absorbent flows were held constant, and the most common experimental conditions were selected (inlet SO_2 concentration: 2000 mg m^{-3}, absorbent concentration: 8000 g m^{-3}, and the total amount of absorbent was always greater than the amount required for SO_2 to react). Figs. 7–8 illustrate the analytical results. The resolved peaks are denoted with the ion names and corresponding values whereas the rest are unresolved peaks. The peak areas of sulfate (SO_2^{-4}), sulfite (SO_2^{-3}), and carbonate (CO_2^{-3}) ions were calculated through integration and compared with the peak area of the standard corresponding ion. Subsequently, the concentrations of SO_2^{-4}, SO_2^{-3}, and CO_2^{-3} in both NaOH and Na_2CO_3 absorbents were obtained through the external standard method, as shown in Table 2. The adjusted SO_2 removal efficiencies were calculated according to the data in Table 2, and the SO_2 removal efficiencies of NaOH and Na_2CO_3 were 82% and 79%, respectively. In contrast to the test results using the gas detector, the margins of error were 0.61% and 6.04%, respectively. The chromatography analysis yielded more

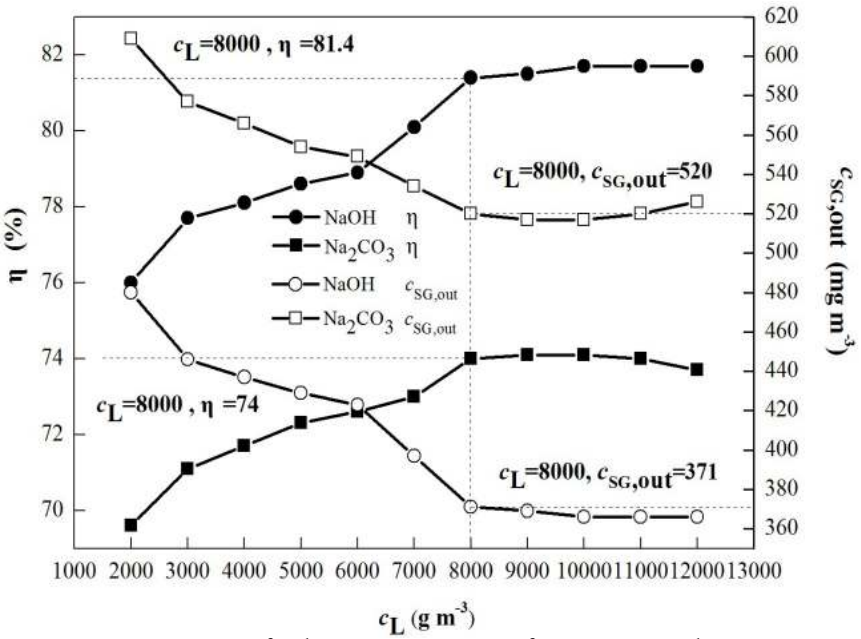

(Q_G= 60 m^3 h^{-1}, $c_{SG,in}$= 2000 mg m^{-3}, Q_L= 800 L h^{-1})

Fig. 5. Effect of absorbent concentration on desulfurization rate.

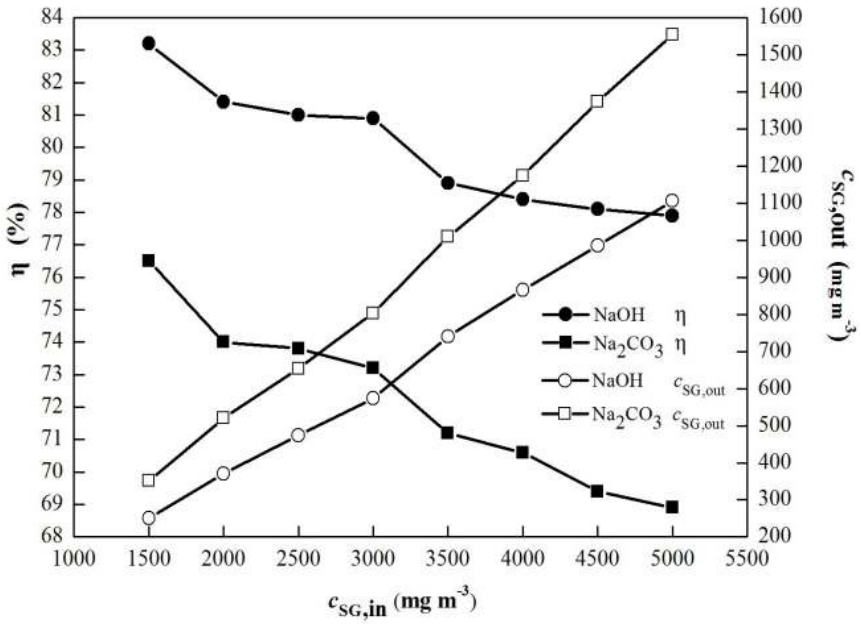

(Q_G= 60 m^3 h^{-1}, Q_L= 800 L h^{-1}, c_L= 8000g m^{-3})

Fig. 6. Effect of inlet SO_2 concentration on SO_2 removal efficiency.

favourable results than the gas detector did; the errors were caused by the difference in the accuracy of the measuring methods.

Effect of Total Gas Flow on SO_2 Removal Efficiency and Pressure Drop

This study examined the effects of total gas flow on SO_2 removal efficiency when the inlet SO_2 concentration, absorbent flow, and absorbent concentration were held constant and the total amount of absorbent was always greater than the amount required for the SO_2 to react. Fig. 9 illustrates the experimental results and demonstrates that η continued to increase as the inlet total gas flow increased from 43 m^3 h^{-1} to 86 m^3 h^{-1}. The maximum η when NaOH and Na_2CO_3 were used as the absorbents were 85.4% and 78.1%, respectively. The SO_2 concentration in the tail gas decreased as the total gas flow increased. The minimum SO_2 concentrations in the tail gas when NaOH and Na_2CO_3 were used as the absorbents were 291 mg m^{-3} and 437 mg m^{-3}, respectively. This experimental result could be interpreted

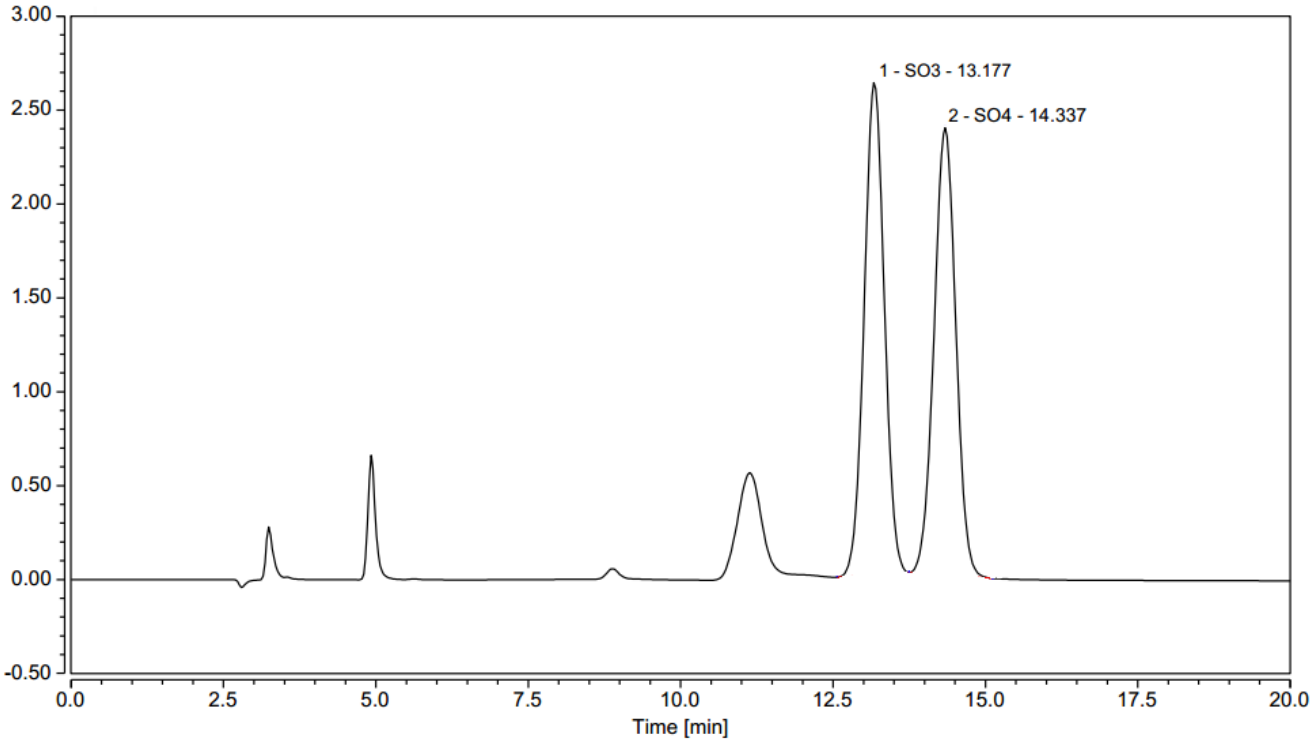

Fig. 7. Sulfite and Sulfate ion distribution chromatogram of NaOH absorbent after reaction.

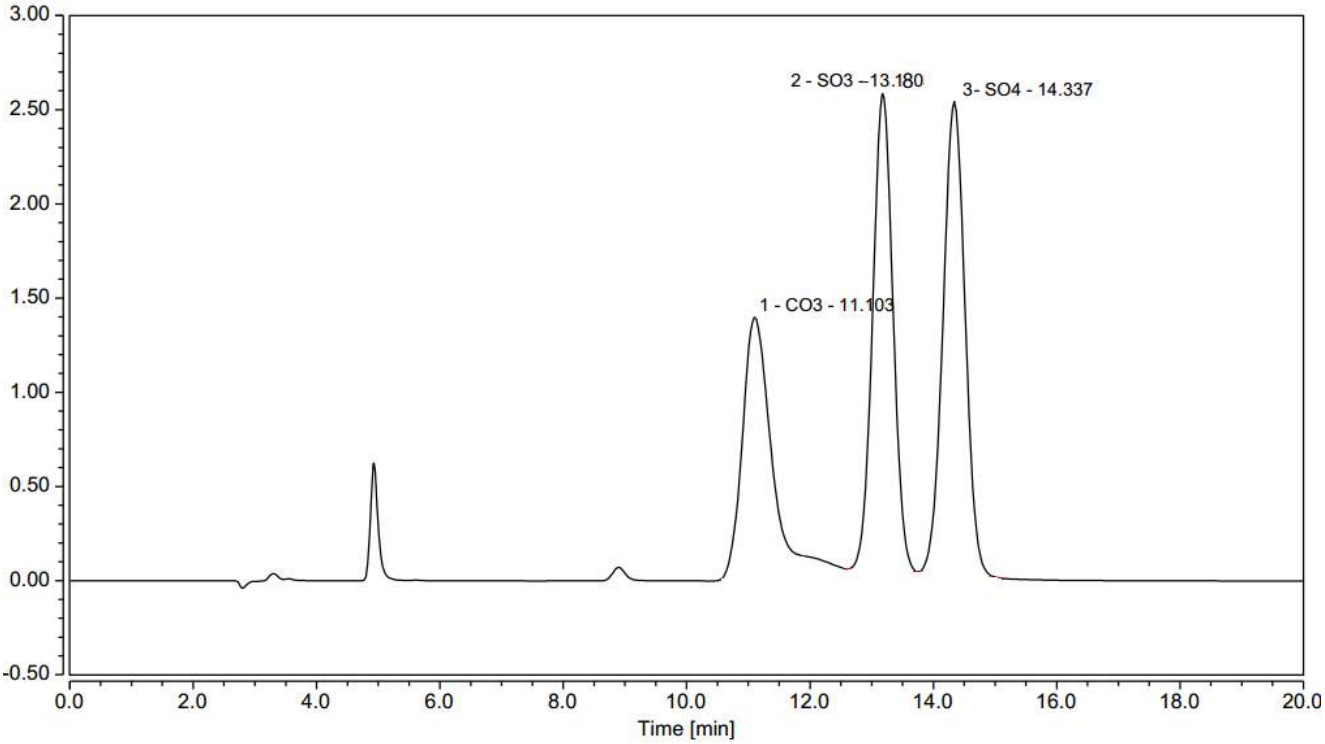

Fig. 8. Carbonate, Sulfite and Sulfate ion distribution chromatogram of Na_2CO_3 absorbent after reaction.

Table 2. DX-600 chromatography analysis.

Type of ion	CO_3^{2-} (mg L^{-1})	SO_3^{2-} (mg L^{-1})	SO_4^{2-} (mg L^{-1})
NaOH absorbent	—	1406.38	438.50
Na_2CO_3 absorbent	3933.70	1343.06	462.03

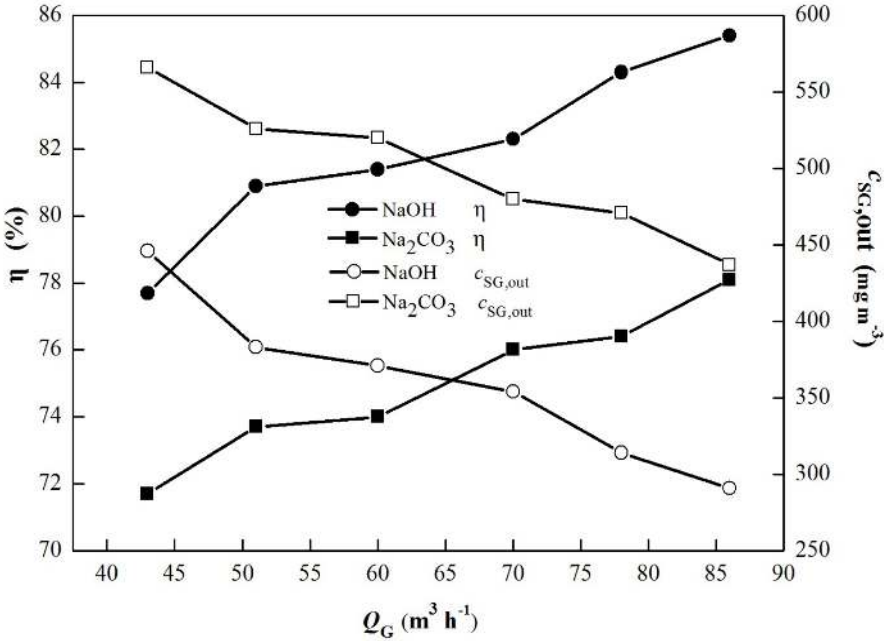

($c_{SG,in}$= 2000 mg m^{-3}, Q_L= 800 L h^{-1}, c_L= 8000 g m^{-3})

Fig. 9. Effect of total gas flow on SO_2 removal efficiency.

as two contrasting phenomena. First, as the total gas flow increased, the absorbent droplets generated by the cyclonic flow field decreased in size, thereby improving the atomization and increasing the mass transfer area between the SO_2 molecules and absorbent droplets. The droplet surfaces were continuously renewed, resulting in a decreased SO_2 concentration in the tail gas and increased η. Conversely, as the total gas flow increased, the duration that the mixture gas stayed in the separator decreased, resulting in decreased reactions between the SO_2 molecules and the absorbents and decreased η. The experimental results revealed that the first phenomenon dominated the second one.

Fig. 10 demonstrates that the air pressure drop of the separator, Δp, and Δp difference increased significantly as the total gas flow increased from 43 m^3 h^{-1} to 86 m^3 h^{-1}. This result is consistent with that of Gu *et al*. (2016). As the density of Na_2CO_3 is slightly higher than that of NaOH, when the total gas flow $\leq$ 70 m^3 h^{-1}, pressure drop of NaOH and Na_2CO_3 was almost the same, when the total gas flow $\geq$ 70 m^3 h^{-1}, pressure drop of Na_2CO_3 was slightly higher than that of NaOH. The greater the pressure drop in the device was, the greater the energy consumption was. The actual gas processed is generally subject to economic calculations. The unique structure of the separator in the present study can improve the SO_2 removal efficiency in practice through a serial connection, or prevent an increase in air pressure or decrease in SO_2 removal efficiency through parallel connections and increased flue gas capacity.

Effect of Absorbent Flow on SO_2 Removal Efficiency

This study examined the effects of absorbent flow on SO_2 removal efficiency when the total gas flow, inlet SO_2 concentration, and absorbent concentration were held constant and the total amount of the absorbent was always greater than the amount required for SO_2 to react. Fig. 11 illustrates the experimental results, demonstrating that η increased as the inlet absorbent flow increased from 600 L h^{-1} to 1100 L h^{-1}. When the absorbent flow reached 1000 L h^{-1}, the change in η flattened out. The maximum η when NaOH and Na_2CO_3 were used as the absorbents were 84.9% and 77.3%, respectively. In addition, the SO_2 concentration in the tail gas decreased as the absorbent flow increased. When the absorbent flow was increased to 1000 L h^{-1}, the change in SO_2 concentration in the tail gas stabilised. The minimum SO_2 concentrations in the flue gas when NaOH and Na_2CO_3 were used as the absorbents were 303 mg m^{-3} and 454 mg m^{-3}, respectively. As the absorbent flow increased, the absorbent droplets generated by the cyclonic flow field rapidly increased. The increased reactions between the SO_2 molecules and the droplets decreased the SO_2 concentration in the tail gas and increased η. In addition, as the absorbent flow increased, the increased injecting velocity strengthened the turbulence. Consequently, the stronger absorption led to the decrease of the SO_2 concentration in the tail gas and an increase of η.

CONCLUSIONS

This study conducted a WFGD experiment on an SO_2–air mixture at room temperature using a gas cyclone–liquid jet absorption separator and NaOH and Na_2CO_3 as absorbents. The SO_2 removal efficiency increased as the absorbents concentration increased and stabilised at 8000 g m^{-3}. The SO_2 removal efficiency decreased as the inlet SO_2 concentration increased. The SO_2 removal efficiency increased as the inlet total gas flow increased. The SO_2 removal efficiency increased as the absorbent flow increased and stabilised at 1000 L h^{-1}.

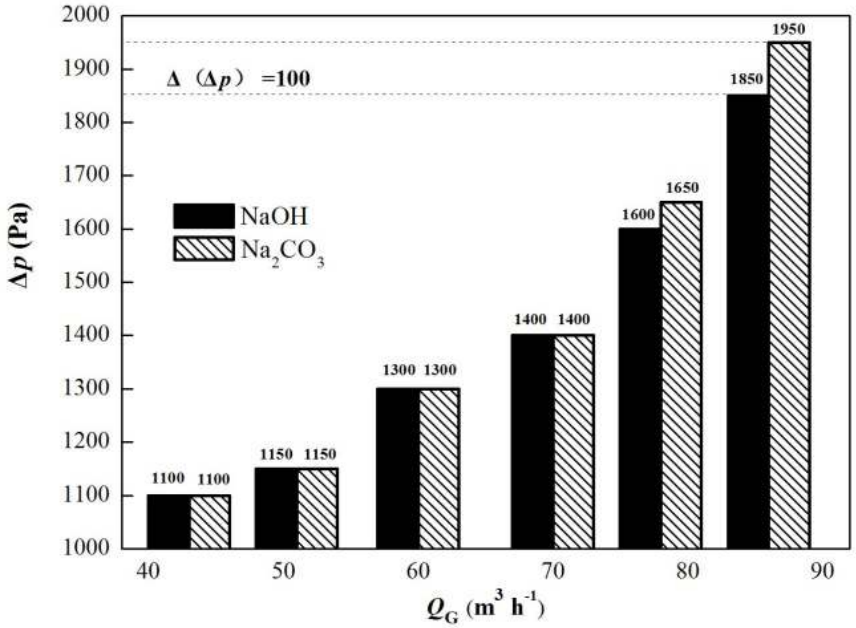

($c_{SG,in}$ = 2000 mg m^{-3}, Q_L = 800 L h^{-1}, c_L = 8000 g m^{-3})

Fig. 10. Effect of total gas flow on pressure drop.

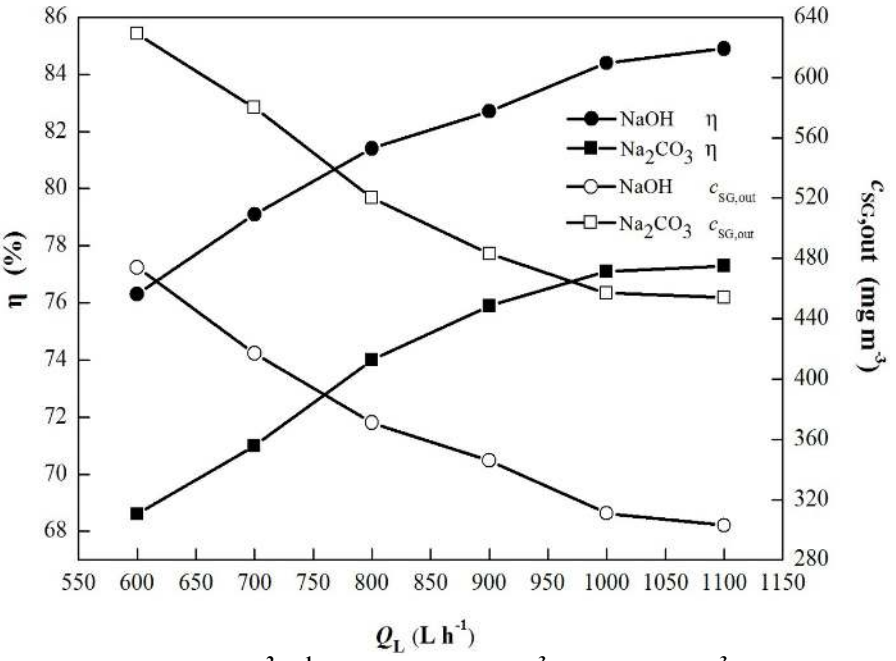

(Q_G = 60 m^2 h^{-1}, $c_{SG,in}$ = 2000 mg m^{-3}, c_L = 8000 g m^{-3})

Fig. 11. Effect of absorbent flow on SO_2 removal efficiency.

The WFGD experiment was conducted at a flue gas flow of 50–85 m^3 h^{-1}, inlet SO_2 concentration of 1500–3000 mg m^{-3}, absorbent flow of 800 L h^{-1}, and absorbent concentration at 8000 g m^{-3}. The maximum SO_2 removal efficiencies of NaOH and Na_2CO_3 were 85% and 77%, respectively. Under identical experimental conditions, the changes in SO_2 removal efficiencies of NaOH and Na_2CO_3 exhibited essentially identical trends, in which that of NaOH was 5%–8% greater than that of Na_2CO_3.

ACKNOWLEDGMENTS

We would like to express our thanks for the sponsorship of National Key Research and Development Program of China (2016YFC0204500), National Natural Science Foundation of China (51608203), Shanghai Rising-Star Program (17QB1400300), and Science and Technology Commission of Shanghai Municipality (16dz1206400).

REFERENCES

Bao, J., Yang, L. and Song, S. (2012). Separation of fine particles from gases in Wet Flue Gas Desulfurization system using a cascade of double towers. *Energy Fuels* 26: 2090–2097.

Bjerle, I., Bengtsson, S. and Farnkvist, R. (1972). Absorption of SO_2 in $CaCO_3$ slurry in a laminar jet absorber. *Chem. Eng. Sci.* 27: 1853–1861.

Bogodage, S.G. and Leung, A.Y.T. (2016). Improvements of the cyclone separator performance by down-comer tubes. *J. Hazard. Mater.* 311: 100–114.

Brogren, C. and Karlsson, H.T. (1997). A model for prediction of limestone dissolution in wet flue gas desulfurization applications. *Ind. Eng. Chem. Res.* 36: 3889–3897.

Chang, G., Song, C. and Wang, L. (2011). A modeling and experimental study of flue gas desulfurization in a dense phase tower. *J. Hazard. Mater.* 189: 134–140.

Chang, M.B., Lee, H.M. and Wu, F. (2004). Simultaneous removal of nitrogen oxide/nitrogen dioxide/sulfur dioxide from gas streams by combined plasma scrubbing technology. *J. Air Waste Manage. Assoc.* 54: 941–949.

Cui, J., Chen, X. and Gong, X. (2010). Numerical study of gas-solid flow in a radial-inlet structure cyclone separator. *Ind. Eng. Chem. Res.* 49: 5450–5460.

Dudek, S.A., Cohara, W.F., Rogers, J.A. (199). Computational Fluid Dynamics (CFD) Model for Predicting Two-Phase Flow in a Flue-Gas-Desulfurization Wet Scrubber. EPRI-DOE-EPA Combined Utility Air Pollutant Control Symposium. August 16–20, 1999, Atlanta, Georgia, U.S.A.

Gong, Y. and Yang, Z. (2011). Corrosion evaluation of one dry desulfurization equipment – Circulating fluidized bed boiler. *Mater. Des.* 32: 671–681.

Gu, X., Song, J. and Wei, Y. (2016). Experimental study of pressure fluctuation in a gas-solid cyclone separator. *Powder Technol.* 22: 217–225.

Klimont, Z., Smith, J.S. and Cofala, J. (2013). The last decade of global anthropogenic sulfur dioxide: 2000-2011 emissions. *Environ. Res. Lett.* 8: 1–6.

Kobayashi, N., Tsutsumi, Y. and Itaya, Y. (2016). Effect of coexistent gases on desulfurization using activated coke in a gasification process. *J. Chem. Eng. Jpn.* 49: 720–727.

Lian, Z., Luo, Z. and Yuan, L. (2004). Corrosion investigation of ammonia flue gas desulfurization. *Mater. Perform.* 54: 941–949.

Ma, L., Yang, Q. and Huang, Y. (2013). Pilot Test on the removal of coke powder from quench oil using a hydrocyclone. *Chem. Eng. Technol.* 36: 696–702.

Ma, L., Wu, J. and Zhang, Y. (2014). Study and application of a cyclone for removing amine droplets from recycled hydrogen in a hydrogenation unit. *Aerosol Air Qual. Res.* 14: 1675–1684.

Michalski, J. (2000). Aerodynamic characteristics of flue gas desulfurization spray towers-polydispersity consideration. *Ind. Eng. Chem. Res.* 39: 3314–3324.

Peng, C., Guo, R. and Fang, X.C. (2016). Improving ultra-deep desulfurization efficiency by catalyst stacking technology. *Catal. Lett.* 146: 701–709.

Pisani, R. and Moraes, D. (2004). Removal of sulfur dioxide from a continuously operated binary fluidized bed reactor using inert solids and hydrated lime. *J. Hazard. Mater.* 109: 183–189.

Qin, L., Han, J. and Deng, Y. (2016). Industrial experimental study on SO_2 removal during novel integrated sintering flue gas desulfurization process. *Fresenius Environ. Bull.* 25: 384–390.

Sada, E. (1981). Desulfurization by limestone slurry with added magnesium sulfate. *Chem. Eng. J.* 22: 133–141.

Safikhani, H. and Mehrabian, P. (2016). Numerical study of flow field in new cyclone separators. *Adv. Powder. Technol.* 27: 379–387.

Sai, J., Wu, S. and Xu, R. (2007). Mass transfer and reaction process of the wet desulfurization reactor with falling film by cross-flow scrubbing. *Korean J. Chem. Eng.* 24: 481–488.

Strock, T. and Gohara, W. (1994). Experimental approach and techniques for the scrubber fluid mechanics. *Chem. Eng. Sci.* 49: 4667–4679.

Sun, Z., Wang, S. and Zhou, Q. (2010). Experimental study on desulfurization efficiency and gas-liquid mass transfer in a new liquid–screen desulfurization system. *Appl. Energy*. 87: 1505-1512.

Uchida, S. and Ariga, O. (1985). Absorption of sulfur dioxide into limestone slurry in a stirred tank. *Chem. Eng. Sci.* 63: 778–783.

Vincent, L., Li, G. and Song, C. (2012). A review of electrochemical desulfurization technologies for fossil fuels. *Fuel Process. Technol.* 98: 30–38.

Wang, S.J., Zhu, P. and Zhang, G. (2015). Numerical simulation research of flow field in ammonia-based wet flue gas desulfurization tower. *J. Energy Inst.* 88: 284–291.

Watson, G.B., Gohara, W.F. and Chaney, L.J. (1999). Advanced Low-Pressure-Drop Tower Inlet Design. EPRI-DOE-EPA Combined Utility Air Pollutant Control Symposium, August 16–20, 1999. Atlanta, Georgia, U.S.A.

Zhang, Q., Gui, K. and Wang, X. (2016). Effects of magnetic fields on improving mass transfer in flue gas desulfurization using a fluidized bed. *Heat Mass Transfer.* 52: 331–336.

Zhang, T., Liu, C. and Guo, K. (2016). Analysis of flow field in optimal cyclone separators with hexagonal structure using mathematical models and computational fluid dynamics simulation. *Ind. Eng. Chem. Res.* 55: 351–365.

Zhang, Y.H., Liu, A.L and Ma, L. (2016). Acid mist cyclone separation experiment on the hydrochloric acid regeneration system of a cold rolling steel plant. *Aerosol Air Qual. Res.* 16: 2287–2293.

Zhu, J., Ye, S. and Bai, J. (2015). A concise algorithm for calculating absorption height in spray tower for wet limestone-gypsum flue gas desulfurization. *Fuel Process. Technol.* 129: 15–23.

Received for review, December 27, 2016
Revised, April 11, 2017
Accepted, April 16, 2017